Title
In situ study of the electronic structure of atomic layer deposited oxide ultrathin films upon oxygen adsorption using ambient pressure XPS

Journal
Catalysis Science & Technology, 6(18)

ISSN
2044-4753

Authors
Mao, Bao-Hua
Crumlin, Ethan
Tyo, Eric C
et al.

Publication Date
2016

DOI
10.1039/c6cy00575f

Peer reviewed

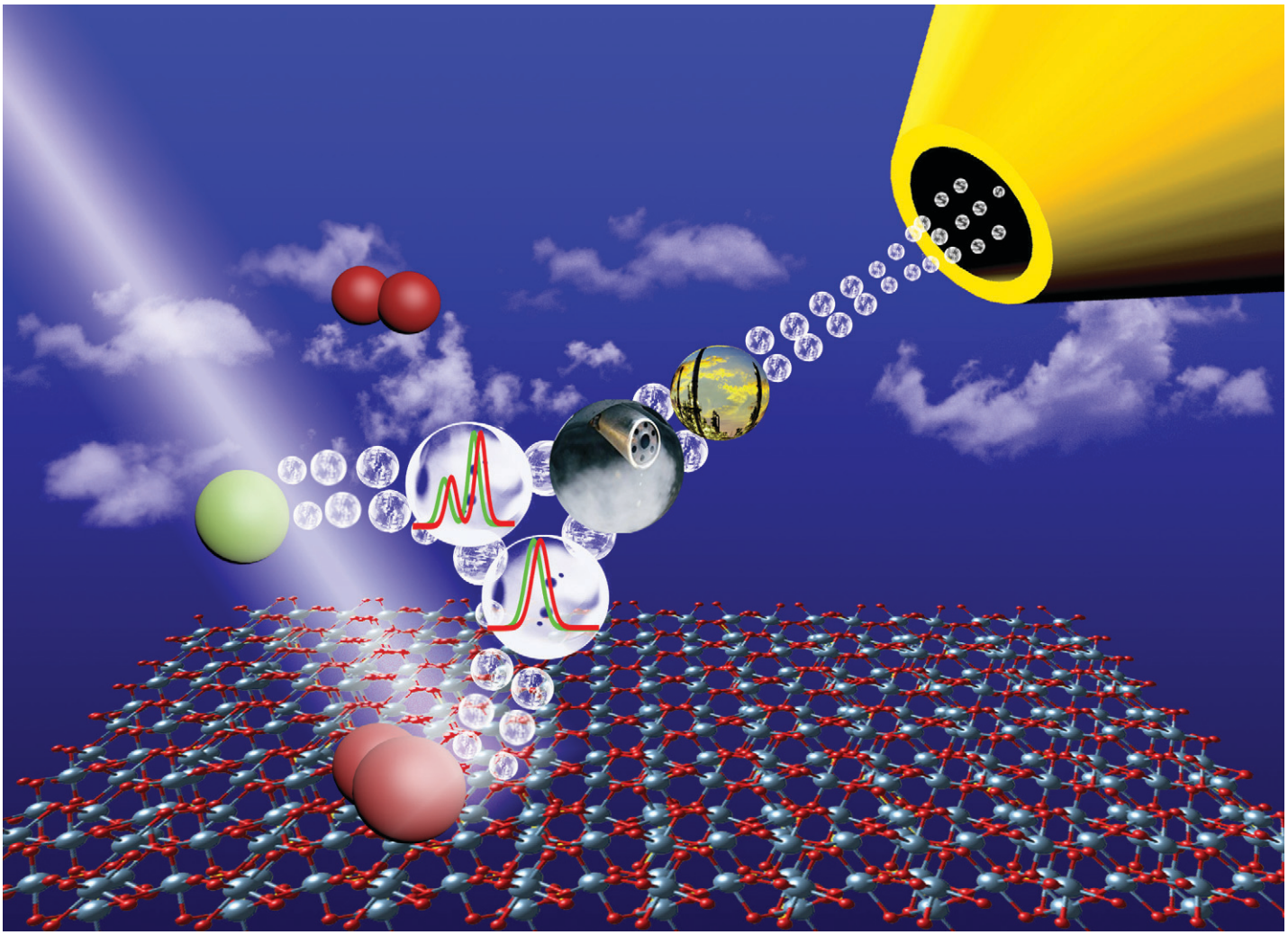

Showcasing research from the Shanghai Institute of Microsystem and Information Technology, Chinese Academy of Sciences, China.

In situ study of the electronic structure of atomic layer deposited oxide ultrathin films upon oxygen adsorption using ambient pressure XPS

The electronic structure of metal oxide ultrathin films was studied using ambient pressure XPS in oxygen and argon atmosphere. The interactions between thin oxide and adsorbed oxygen can be effectively detected through electronic structure and electron affinity measurements.

As featured in:

See Yimin Li, Sui-Dong Wang, Zhi Liu *et al.*, *Catal. Sci. Technol.*, 2016, **6**, 6778.

ROYAL SOCIETY OF CHEMISTRY

www.rsc.org/catalysis

Registered charity number: 207890

Catalysis Science & Technology

PAPER

View Article Online
View Journal | View Issue

CrossMark click for updates

Cite this: *Catal. Sci. Technol.*, 2016, **6**, 6778

In situ study of the electronic structure of atomic layer deposited oxide ultrathin films upon oxygen adsorption using ambient pressure XPS†

Bao-Hua Mao,[abc] Ethan Crumlin,[c] Eric C. Tyo,[d] Michael J. Pellin,[d] Stefan Vajda,[defg] Yimin Li,*[bh] Sui-Dong Wang*[a] and Zhi Liu*[bch]

Received 16th March 2016,
Accepted 20th July 2016

DOI: 10.1039/c6cy00575f

www.rsc.org/catalysis

In this work, ambient pressure X-ray photoelectron spectroscopy (APXPS) was used to investigate the effect of oxygen adsorption on the band bending and electron affinity of Al_2O_3, ZnO and TiO_2 ultrathin films (~1 nm in thickness) deposited on a Si substrate by atomic layer deposition (ALD). Upon exposure to oxygen at room temperature (RT), upward band bending was observed on all three samples, and a decrease in electron affinity was observed on Al_2O_3 and ZnO ultrathin films at RT. At 80 °C, the magnitude of the upward band bending decreased, and the change in the electron affinity vanished. These results indicate the existence of two surface oxygen species: a negatively charged species that is strongly adsorbed and responsible for the observed upward band bending, and a weakly adsorbed species that is polarized, lowering the electron affinity. Based on the extent of upward band bending on the three samples, the surface coverage of the strongly adsorbed species exhibits the following order: $Al_2O_3 > ZnO > TiO_2$. This finding is in stark contrast to the trend expected on the surface of these bulk oxides, and highlights the unique surface activity of ultrathin oxide films with important implications, for example, in oxidation reactions taking place on these films or in catalyst systems where such oxides are used as a support material.

Introduction

Ultrathin oxide films with thicknesses of approximately several nanometers are key components in many important applications, such as gas sensing, passivation layers and catalysis.[1] For example, ultrathin TiO_2 films have been used as the protective layer on semiconductor photocatalysts, significantly improving their photocorrosion resistance in photoelectrochemical (PEC) water splitting.[2,3] The deposition of a thin oxide layer creates a new type of solid/solid interface, which inevitably alters the energy-level alignment in the interfacial region and affects the charge transfer process during redox reactions on the catalyst surface. Furthermore, because of the ultrathin thickness and the abundance of surface defects, the energy level alignment of the oxide film is affected by a variety of environmental phenomena such as surface adsorption at different pressures and temperatures. Therefore, developing reliable *in situ* characterization techniques for energy level alignment at the oxide surface/interface is vital for applications using ultrathin oxide films.

Unlike bulk materials, ultrathin films have distinctive electronic structures because of their restrained dimension, different atomic structures and abundant surface defects.[4,5] However, the electronic structure of ultrathin films has not been explored as intensively as that of the bulk form. For practical applications, understanding the electronic structure changes of ultrathin films under different environments is crucial. One important aspect is the influence of gas molecule adsorption on the electronic structure.[6–8] Chen *et al.* discovered that this adsorption induced an electronic structure change in semiconductors known as "surface transfer doping".[9–11] Many techniques have been applied to study the electronic structure, including X-ray photoelectron spectroscopy (XPS) and ultraviolet photoelectron spectroscopy (UPS).[12,13] Conventional XPS and UPS are limited to ultrahigh

[a] *Institute of Functional Nano & Soft Materials (FUNSOM), Jiangsu Key Laboratory for Carbon-Based Functional Materials & Devices, Soochow University, Suzhou, Jiangsu 215123, People's Republic of China. E-mail: wangsd@suda.edu.cn*
[b] *State Key Laboratory of Functional Materials for Informatics, Shanghai Institute of Microsystem and Information Technology, Chinese Academy of Sciences, Shanghai 200050, People's Republic of China. E-mail: zliu2@mail.sim.ac.cn, yml@mail.sim.ac*
[c] *Advanced Light Source, Lawrence Berkeley National Laboratory, Berkeley, California 94720, USA*
[d] *Materials Science Division, Argonne National Laboratory, Argonne, Illinois 60439, USA*
[e] *Nanoscience & Technology Division, Argonne National Laboratory, Argonne, Illinois 60439, USA*
[f] *Department of Chemical and Environmental Engineering, School of Engineering & Applied Science, Yale University, New Haven, Connecticut 06520, USA*
[g] *Institute of Molecular Engineering, The University of Chicago, 5747 South Ellis Avenue, Chicago, IL, 60637, USA*
[h] *School of Physical Science and Technology, ShanghaiTech University, Shanghai 200031, China*

† Electronic supplementary information (ESI) available. See DOI: 10.1039/c6cy00575f

vacuum (UHV) conditions. Therefore, an appropriate technique allowing for *in situ* studies of the electronic structure of ultrathin films under near ambient conditions is of high importance.

Ambient pressure XPS (APXPS) can measure the core level spectra of materials and gas molecules *in situ* under near ambient pressure conditions, as shown in Fig. 1a. APXPS has been successfully applied to study the band bending change of materials upon gas adsorption.[14,15] Fig. 1b shows how the surface band bending change upon gas exposure is reflected in core level binding energy (BE_{Samp}) changes in the samples. In 2013, Axnanda *et al.* developed a work function measurement method by recording the core level spectrum of Ar gas in the vicinity of a sample using APXPS and successfully applied this method to measure the work function of PbS quantum dots.[16] The electronic levels of the gas-phase molecules are referenced to the vacuum level (VL). In the vicinity of the sample surface, the core level BE of gas molecules (BE_{Gas}) will shift as the sample's VL changes. Thus, a sample work function change can be measured using the change in BE_{Gas}. This ability to measure changes in work function, band bending, and electron affinity upon gas adsorption makes APXPS an ideal technique to study gas adsorption processes on different surfaces and provide information on the electronic structure in more realistic environments than a vacuum.

In this study, we chose Al_2O_3, TiO_2 and ZnO ultrathin films created *via* atomic layer deposition (ALD) as model systems and monitored their interactions with oxygen *via* changes in their subsequent electronic structure changes using APXPS. By measuring the core level BEs of the samples and gas molecules, the work functions and band bending of these materials were obtained under both oxygen and oxygen-free conditions. Based on these band bending and work function results, we also deduced the electron affinity changes, which were strongly influenced by the adsorbed oxygen species.[17] In addition, we also studied the effect of temperature on the oxygen adsorption behavior and the aforementioned electronic properties. This work provides experimental information that can improve our understanding of oxygen adsorption on different metal oxide ultrathin films under environments relevant to practical applications, which is crucial for the design of new catalysts and electronic devices.

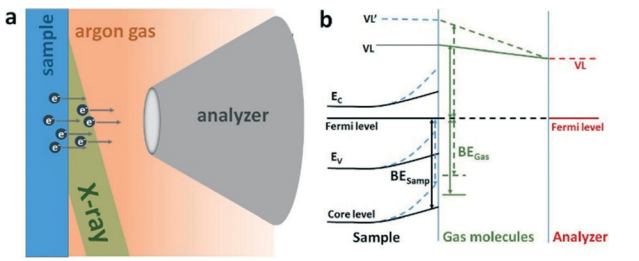

Fig. 1 (a) Schematic diagram of the experimental setup with photoelectrons emitted from both the sample and Ar gas molecules in the vicinity of the sample surface. (b) Schematic diagram of the band bending and work function measurement using APXPS. BE_{Samp} and BE_{Gas} are the core level BEs of the sample and gas molecules, respectively. VL and VL′ are the vacuum levels of the sample before and after gas adsorption. E_C is the edge of the conduction band and E_V is the edge of the valence band.

Experimental

The Al_2O_3, TiO_2, and ZnO ultrathin films were prepared *via* ALD on top of an n-type (phosphorus-doped) Si (110) wafer using a custom viscous flow ALD reactor. The thicknesses of the Al_2O_3, TiO_2, and ZnO films were 0.74 nm, 1.88 nm, and 0.78 nm, respectively. A detailed description of the fabrication procedure can be found in previous reports.[18–20]

The APXPS experiments were performed at the bending-magnet beamline 9.3.2 of the Advanced Light Source, Lawrence Berkeley National Laboratory. This beamline can perform XPS experiments under different gas atmospheres with pressures up to 1 Torr. A detailed description of the APXPS setup can be found in previous reports.[21] The samples were mounted on a sample holder along with a piece of gold foil for energy calibration. The XPS spectra of all samples and Ar were recorded under pure Ar and mixed Ar/O_2 atmospheres to study the effect of oxygen adsorption. The Ar in the analysis chamber was used as the reference for work function measurement. Ar, an inert gas, was chosen for this purpose because of its non-interacting nature with samples.[16] All XPS peak positions were calibrated using Au $f_{7/4}$ (84 eV). Two individual UHV leak valves were used to introduce oxygen (Air Gas, UHP) and Ar (Air Gas, UHP) to the analysis chamber. A calibrated Baratron gauge was used to monitor the total pressure in the analysis chamber. The photon energy of the X-ray used in this experiment was 770 eV.

Results and discussion

First, the core level spectra of interest of the ultrathin films were collected to measure their band bending. As shown in Fig. 1b, band bending is caused by the electric field in depletion regions because of charge transfer between the adsorbed molecules and the semiconductor surface. This electric field and potential change also affect the core level of the semiconductor, and thus, the core level BE change can be used to calculate the band bending change.[15,22,23] The core level BEs of Ar gas molecules in the vicinity of the samples were measured to determine the work function changes. The samples were connected electronically with the analyzer and therefore, their Fermi levels were equivalent to that of the analyzer during the XPS measurement. When the sample work function changes, the sample's VL will also change. We can directly correlate the core level XPS BE change with the work function change of a sample as described previously.[24] For the calibration, different bias voltages (−2 V to +2 V) were applied to highly oriented pyrolytic graphite (HOPG) to obtain the relationship between the Ar 2p BE and the sample work function (Fig. S2, ESI†). HOPG was chosen for this purpose because of its inert nature upon gas exposure. Using this method, the

linear relationship of the Ar 2p BE with the sample work function was obtained, as shown in eqn (1):

$$\Phi_{samp} = -1.03BE_{gas} + 256.24 \quad (1)$$

where Φ_{samp} is the sample work function, and BE_{gas} is the BE of Ar $2p_{3/2}$.

After establishing the relationship between the Ar 2p BE and the sample work function, we measured the XPS spectra of the Al_2O_3 ultrathin film at room temperature (RT). As shown in Fig. 2a, the Al 2p BE was 75.85 eV in 200 mTorr Ar, slightly higher than that of bulk Al_2O_3.[25] After introducing 200 mTorr oxygen, the BE of Al 2p decreased by 0.61 eV to 75.24 eV. The lowering of the Al 2p BE in Al_2O_3 is not attributed to an Al chemical state change because in this case, under an oxygen environment, the Al 2p BE should shift to a higher value, and not exhibit the downshift observed here. Another interesting phenomenon is that the BE change was reversible when the introduction of oxygen and Ar was alternated, which is consistent with the results of our previous work.[14] This lowering of the BE upon exposure to oxygen resulted from the surface band bending effect.[15,26] We used the measured Ar 2p BE to determine the work function of the sample. As shown in Fig. 2b, the BE of Ar $2p_{3/2}$ was 245.51 eV in the absence of oxygen. According to eqn (1), the work function of Al_2O_3 was 3.36 eV under this condition. However, after oxygen introduction, the BE of Ar $2p_{3/2}$ shifted to 245.04 eV, and the work function of Al_2O_3 was determined to be 3.84 eV, corresponding to an increase of 0.48 eV resulting from oxygen adsorption.

To further investigate the effect of temperature on oxygen adsorption, XPS of the Al_2O_3 ultrathin film was performed at 80 °C. This temperature was chosen because it is a frequently applied temperature for various catalysis reactions involving Al_2O_3 film supports to prevent catalyst particle aggregation.[18] As shown in Fig. 2c, the BE of Al 2p was 75.62 eV at 80 °C under 200 mTorr Ar. After introducing 200 mTorr oxygen, the BE decreased to 75.27 eV, indicating an upward band bending of 0.35 eV upon oxygen adsorption. The BE of Ar $2p_{3/2}$ was 245.38 eV (Fig. 2d) in the absence of oxygen at 80 °C, and thus, the work function of the Al_2O_3 film was 3.49 eV. After oxygen was introduced, the BE of Ar $2p_{3/2}$ was 245.07, corresponding to a work function of 3.81 eV, and an increase of 0.32 eV after oxygen adsorption.

According to the literature, two types of oxygen chemisorption exist: strong chemisorption and weak chemisorption.[7] Substantial work has been conducted to investigate the electronic structure changes caused by these two types of oxygen chemisorption.[6,27,28] Geistlinger *et al.*[7] demonstrated that strongly chemisorbed species could undergo delocalized charge transfer with the substrate to create a depletion layer, thereby resulting in band bending;[6,7] however, they also reported that these species exert relatively little influence on the electron affinity change. In contrast, weakly chemisorbed species can form dipoles on the surface and subsequently vary the surface electron affinity, but they typically do not change the band bending significantly. As shown in Fig. 3, both the band bending and electron affinity changes contribute to the work function change and their relationship can be described by eqn (2):

$$\Delta\Phi = \Delta V_s + \Delta\chi \quad (2)$$

where $\Delta\Phi$ is the change in the work function, ΔV_s is the change in the band bending and $\Delta\chi$ is the change in the electron affinity.[17]

In our study, the Al_2O_3 ultrathin film exhibited upward band bending after oxygen exposure at both RT and 80 °C. As described above, this result indicates the existence of strongly chemisorbed oxygen species on the Al_2O_3 ultrathin film surface at both temperatures; these species undergo delocalized charge transfer with the substrate and create a depletion layer that results in band bending.[6,7] However, bulk Al_2O_3

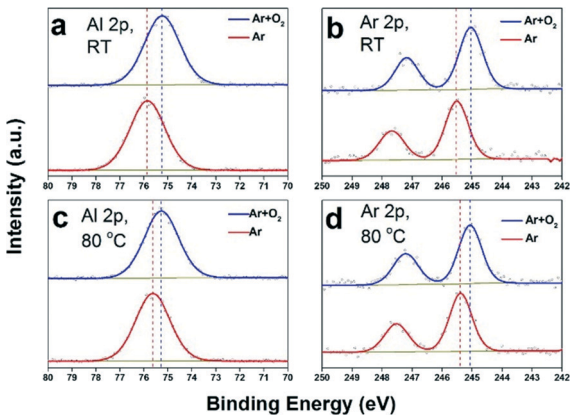

Fig. 2 XPS spectra of Al 2p and Ar 2p on Al_2O_3 ultrathin films under Ar (red curves) and Ar + O_2 atmospheres (blue curves): (a) Al 2p of Al_2O_3 at RT, (b) Ar 2p of gas phase Ar at RT, (c) Al 2p of Al_2O_3 at 80 °C and (d) Ar 2p of gas phase Ar at 80 °C.

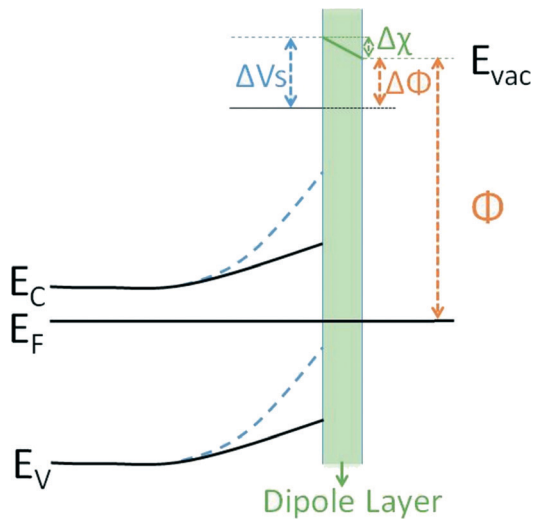

Fig. 3 Scheme of the electronic structure change of n-type semiconductors upon oxygen adsorption. ΔV_s, $\Delta\chi$ and $\Delta\Phi$ are the changes in the band bending, electron affinity and work function, respectively.

with a well-defined surface structure is known to be a fairly inert oxide exhibiting no oxygen adsorption at temperatures below 500 °C.[29] The distinctive oxygen adsorption behavior of the ultrathin film and bulk Al_2O_3 can be attributed to the abundant defects on the surface of Al_2O_3 ultrathin films.[30–32] The values of the change of band bending after introducing oxygen at these two temperatures were also different: 0.61 eV at RT *vs.* 0.32 eV at 80 °C. We attribute this diminished band bending effect at 80 °C to either increased oxygen desorption or increased carrier density in the Al_2O_3 ultrathin film at higher temperature.[33]

Using eqn (2), the electron affinity change of the Al_2O_3 ultrathin film was determined to be −0.13 eV upon oxygen adsorption at RT (Table 1). As proposed by Geistlinger, such an electron affinity change can be attributed to weakly chemisorbed species undergoing localized charge transfer with the oxide surface.[6,7] The localized charge transfer between the molecules and the adsorption site on the surface will create dipoles and generate a potential drop across the dipole layer that is equal to the electron affinity change. However, at 80 °C, the electron affinity change of the Al_2O_3 film before and after oxygen exposure was only −0.03 eV (Table 1), indicating that almost no weakly chemisorbed oxygen was present under these conditions. This finding can be attributed to the relatively weak binding of these species with the substrate and their ready desorption at higher temperatures.

In addition to Al_2O_3, we also studied oxygen adsorption on ZnO and TiO_2 ultrathin films at RT. ZnO and TiO_2 are two semiconductor materials that are widely used for catalysis and devices.[18,34,35] As shown in Fig. 3a, the BE of Zn $3p_{3/2}$ in an Ar atmosphere was 90.48 eV. After the introduction of oxygen, the BE shifted to 90.04 eV, indicating that the adsorption of oxygen on the ZnO film results in an upward band bending of 0.44 eV. The change in the work function was also recorded by measuring the core level spectra of Ar gas in the vicinity of the ZnO film (Fig. 3b). The BE of Ar $2p_{3/2}$ was 245.34 without oxygen and changed to 245.04 eV after the introduction of oxygen. According to eqn (1), the work function of the ZnO film was 3.53 eV under oxygen-free conditions and 3.85 eV after the introduction of oxygen. Thus, oxygen adsorption increases the work function by 0.32 eV.

Similarly, for the TiO_2 film (Fig. 4c), the Ti $2p_{3/2}$ BE was 459.93 eV without oxygen and shifted to 459.62 eV after oxygen introduction, corresponding to a band bending of 0.31 eV on the surface of the TiO_2 film caused by oxygen adsorption. As shown in Fig. 4d, the BE of Ar $2p_{3/2}$ was 245.15 eV near the TiO_2 film surface in an Ar atmosphere, and this value increased to 244.83 eV after oxygen introduction. According to eqn (1), the work function of the TiO_2 film in an Ar atmosphere was 3.73 eV and increased to 4.06 eV after the introduction of oxygen, thus, oxygen adsorption increased the work function by 0.33 eV.

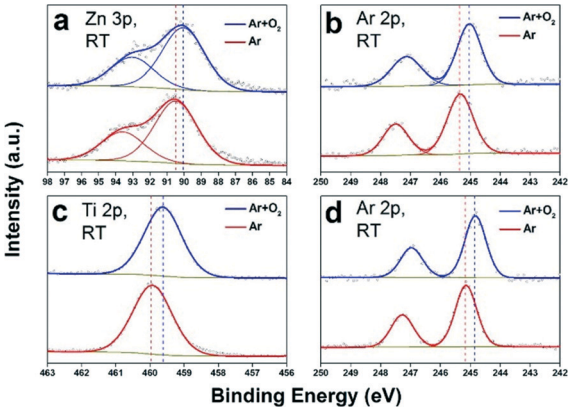

Fig. 4 XPS spectra of the TiO_2 and ZnO ultrathin films under Ar and mixed Ar + O2 atmospheres at room temperature: Zn 3p (a) and Ar 2p (b) of the ZnO sample, and Ti 2p (c) and Ar 2p (d) of the TiO_2 sample.

All of the results from the three tested samples are summarized in Table 1. Upward band bending shifts were observed in all three samples after the introduction of oxygen, indicating that strongly chemisorbed oxygen species formed on all three surfaces. The different band bending observed on different oxide films could be related to the different charge carrier concentrations and amounts of strongly chemisorbed oxygen on the oxide thin films.[17]

According to eqn (2), the electron affinity change for the ZnO ultrathin film was −0.12 eV in the presence of oxygen, similar to that of the Al_2O_3 ultrathin film at RT (Table 1). In contrast, the electron affinity of the TiO_2 ultrathin film showed almost no change after oxygen adsorption at RT, suggesting the absence of weakly chemisorbed oxygen on the TiO_2 surface.

For all three oxide films, oxygen adsorption shifts the band bending at the interfaces upward, indicating the existence of negatively charged surface oxygen species (strongly adsorbed species). The extent of this upward band bending should increase as the surface coverage of the negatively charged oxygen species $O_2^{-\delta}$ and the charge δ on each oxygen species increase. We observed that the magnitude of upward band bending exhibited the following order: Al_2O_3 > ZnO > TiO_2. This ordering indicates that the surface concentration of $O_2^{-\delta}$ on the Al_2O_3 ALD film is much larger than that on the TiO_2 film because more negatively charged oxygen typically adsorbed on TiO_2, leading to a larger δ per adsorbed oxygen.

We also observed that oxygen adsorption on Al_2O_3 and ZnO thin films at RT decreased the surface electron affinity. This decrease suggests that an oxygen species with its dipole pointing away from the surface should be present. The

Table 1 Band bending, work function, and electron affinity changes of metal oxide ultrathin films after oxygen introduction. The electron affinity change was determined using eqn (2) and measurements of the bending and work function changes

Sample and temperature	Band bending change (eV)	Work function change (eV)	Electron affinity change (eV)
Al_2O_3, RT	0.61	0.48	−0.13
Al_2O_3, 80 °C	0.35	0.32	−0.03
ZnO, RT	0.44	0.32	−0.12
TiO_2, RT	0.31	0.33	0.02

disappearance of the electron affinity change at 80 °C shows that this oxygen species is weakly adsorbed.

Conclusions

Based on our APXPS results, two distinctive types of adsorption sites likely exist on ultrathin ALD oxide films and are responsible for the adsorption of two species: electron rich sites at which $O_2^{-\delta}$ adsorbs, and electronegative sites that interact with the lone electron pairs of oxygen atoms in the polarized species with dipoles pointing away from the surface. Estimation of the surface densities of the two adsorption sites based on the surface coverage of oxygen species at RT revealed that the overall surface densities of these sites are very small (on the order of 10^{-2} ML; see the ESI†). Such quantities are very difficult to probe using conventional XPS. However, APXPS band bending and electron affinity measurements can not only reveal the effects of these adsorption sites but also differentiate their different contributions. The surface coverage of the strongly adsorbed species scaled in the following order: $Al_2O_3 > ZnO > TiO_2$. This finding, which is in stark contrast to the trends expected to occur on the surface of the bulk counterpart of these oxides, underlines the unique surface activity of ultrathin oxide films, which may have important implications, for example, in oxidative reactions taking place on these films or in catalyst systems where such oxides are used as a catalyst support.

Acknowledgements

The Advanced Light Source was supported by the Director, Office of Science, Office of Basic Energy Sciences, of the U.S. Department of Energy under Contract No. DE-AC02-05CH11231. This work in China was supported by the National Natural Science Foundation of China (11227902 and 61274019), the Soochow University-Western University Joint Centre for Synchrotron Radiation Research, and the Collaborative Innovation Center of Suzhou Nano Science & Technology. Y. L would like to acknowledge the support from the One Hundred Science Foundation of the Chinese Academy of Sciences. The work at the Argonne National Laboratory was supported by the U.S. Department of Energy (DOE), Office of Science, Basic Energy Sciences, division of Materials Sciences and Engineering under Contract No. DE-AC-02-06CH11357.

References

1 S. M. George, *Chem. Rev.*, 2009, **110**, 111–131.
2 A. Paracchino, N. Mathews, T. Hisatomi, M. Stefik, S. D. Tilley and M. Grätzel, *Energy Environ. Sci.*, 2012, **5**, 8673–8681.
3 B. Seger, D. S. Tilley, T. Pedersen, P. C. Vesborg, O. Hansen, M. Grätzel and I. Chorkendorff, *RSC Adv.*, 2013, **3**, 25902–25907.
4 T. Ohsawa, M. Saito, I. Hamada, R. Shimizu, K. Iwaya, S. Shiraki, Z. Wang, Y. Ikuhara and T. Hitosugi, *ACS Nano*, 2015, **9**, 8766–8772.
5 A. J. Nozik and R. Memming, *J. Phys. Chem.*, 1996, **100**, 13061–13078.
6 T. Sahm, A. Gurlo, N. Barsan and U. Weimar, *Sens. Actuators, B*, 2006, **118**, 78–83.
7 H. Geistlinger, *Sens. Actuators, B*, 1993, **17**, 47–60.
8 D. Kang, H. Lim, C. Kim, I. Song, J. Park, Y. Park and J. Chung, *Appl. Phys. Lett.*, 2007, **90**, 192101.
9 Y. Lu, W. Chen, Y. Feng and P. He, *J. Phys. Chem. B*, 2008, **113**, 2–5.
10 W. Chen, D. Qi, X. Gao and A. T. S. Wee, *Prog. Surf. Sci.*, 2009, **84**, 279–321.
11 W. Chen, S. Chen, D. C. Qi, X. Y. Gao and A. T. S. Wee, *J. Am. Chem. Soc.*, 2007, **129**, 10418–10422.
12 A. Kahn, N. Koch and W. Gao, *J. Polym. Sci., Part B: Polym. Phys.*, 2003, **41**, 2529–2548.
13 H. Ishii, K. Sugiyama, E. Ito and K. Seki, *Adv. Mater.*, 1999, **11**, 605–625.
14 B.-H. Mao, R. Chang, L. Shi, Q.-Q. Zhuo, S. Rani, X.-S. Liu, E. C. Tyo, S. Vajda, S.-D. Wang and Z. Liu, *Phys. Chem. Chem. Phys.*, 2014, **16**, 26645–26652.
15 S. Porsgaard, P. Jiang, F. Borondics, S. Wendt, Z. Liu, H. Bluhm, F. Besenbacher and M. Salmeron, *Angew. Chem., Int. Ed.*, 2011, **50**, 2266–2269.
16 S. Axnanda, M. Scheele, E. Crumlin, B. Mao, R. Chang, S. Rani, M. Faiz, S. Wang, A. P. Alivisatos and Z. Liu, *Nano Lett.*, 2013, **13**, 6176–6182.
17 H. Lüth, *Solid surfaces, interfaces and thin films*, Springer, 2001.
18 Y. Lei, F. Mehmood, S. Lee, J. Greeley, B. Lee, S. Seifert, R. E. Winans, J. W. Elam, R. J. Meyer and P. C. Redfern, *Science*, 2010, **328**, 224–228.
19 M. Groner, F. Fabreguette, J. Elam and S. George, *Chem. Mater.*, 2004, **16**, 639–645.
20 S. Lee, B. Lee, F. Mehmood, S. Seifert, J. A. Libera, J. W. Elam, J. Greeley, P. Zapol, L. A. Curtiss and M. J. Pellin, *J. Phys. Chem. C*, 2010, **114**, 10342–10348.
21 M. E. Grass, P. G. Karlsson, F. Aksoy, M. Lundqvist, B. Wannberg, B. S. Mun, Z. Hussain and Z. Liu, *Rev. Sci. Instrum.*, 2010, **81**, 053106.
22 Z. Zhang and J. T. Yates Jr, *J. Phys. Chem. Lett.*, 2010, **1**, 2185–2188.
23 K. Kakushima, K. Okamoto, M. Adachi, K. Tachi, J. Song, S. Sato, T. Kawanago, P. Ahmet, K. Tsutsui and N. Sugii, *Appl. Surf. Sci.*, 2008, **254**, 6106–6108.
24 C. Heine, M. Hävecker, M. Sanchez-Sanchez, A. Trunschke, R. Schlögl and M. Eichelbaum, *J. Phys. Chem. C*, 2013, **117**, 26988–26997.
25 Y.-C. Kim, H.-H. Park, J. S. Chun and W.-J. Lee, *Thin Solid Films*, 1994, **237**, 57–65.
26 M. Lampimäki, V. Zelenay, A. Křepelová, Z. Liu, R. Chang, H. Bluhm and M. Ammann, *ChemPhysChem*, 2013, **14**, 2419–2425.
27 L. Grządziel, M. Krzywiecki, H. Peisert, T. Chassé and J. Szuber, *Thin Solid Films*, 2011, **519**, 2187–2192.
28 L. Grządziel and M. Krzywiecki, *Thin Solid Films*, 2014, **550**, 361–366.
29 N. Barsan and U. Weimar, *J. Electroceram*, 2001, **7**, 143–167.

30 M. Schmid, M. Shishkin, G. Kresse, E. Napetschnig, P. Varga, M. Kulawik, N. Nilius, H.-P. Rust and H.-J. Freund, *Phys. Rev. Lett.*, 2006, **97**, 046101.
31 E. Ozensoy, C. H. Peden and J. Szanyi, *J. Phys. Chem. B*, 2005, **109**, 15977–15984.
32 J. Toofan and P. Watson, *Surf. Sci.*, 1998, **401**, 162–172.
33 M. Head-Gordon, J. C. Tully, C. T. Rettner, C. B. Mullins and D. J. Auerbach, *J. Chem. Phys.*, 1991, **94**, 1516–1527.
34 S. M. Chou, L. G. Teoh, W. H. Lai, Y. H. Su and M. H. Hon, *Sensors*, 2006, **6**, 1420–1427.
35 R. M. Walton, J. L. Gland and J. W. Schwank, *Surf. Interface Anal.*, 1997, **25**, 76–80.